



Modeling the endophytic fungus *Epicoccum nigrum* action to fight the “olive knot” disease caused by *Pseudomonas savastanoi* pv. *savastanoi* (*Psv*) bacteria in *Olea europea* L. trees.

Cecilia Berardo[†], Iulia Martina Bulai*, Paula Baptista[‡], Teresa Gomes[‡],
Ezio Venturino[†]

[†]Dipartimento di Matematica “Giuseppe Peano”, Università di Torino,
via Carlo Alberto 10, 10123 Torino, ITALY
ezio.venturino@unito.it

*Department of Information Engineering, University of Padova, Italy

CIMO, School of Agriculture, Polytechnic Institute of Bragança,
Campus de Santa Apolónia, 5300-253 Bragança, Portugal

Acknowledgments: Research partially supported by the project “Metodi numerici nelle scienze applicate” of the Dipartimento di Matematica “Giuseppe Peano”.

Also by COST Action: FA 1405 - Food and Agriculture: Using three-way interactions between plants, microbes and arthropods to enhance crop protection and production

OUTLINE

Introduction

The model

The ecosystem's steady states

Simulations

Conclusions

1 Introduction

Olive knot, caused by *Pseudomonas savastanoi* pv. *savastanoi* (*Psv*), is one of the most important diseases of olive crop, produces tumorous galls or knots on stems and branches of olive trees, causing their death or loss of vigour. *Psv* is usually found in olive tree phyllosphere as an epiphyte and/or endophyte.

J. M. Quesada, R. Penyalver, J. Pérez-Panadés, C. I. Salcedo, E. A. Carbonell, M. M. López, Dissemination of *Pseudomonas savastanoi* pv. *savastanoi* populations and subsequent appearance of olive knot disease. Plant Pathology 59: 262-269 (2010).

J. M. Quesada, R. Penyalver, M. M. López, Epidemiology and Control of Plant Diseases Caused by Phytopathogenic Bacteria: The Case of Olive Knot Disease Caused by *Pseudomonas savastanoi* pv. *savastanoi*, Plant Pathology, Dr. Christian Joseph Cumagun (Ed.), ISBN: 978-953-51-0489-6, InTech (2012).



Figure 1: Olive knot disease.



Figure 2: Olive knot disease.



Figure 3: Olive knot disease.



Figure 4: Olive knot disease.

Disease development depends on *Psu* interaction with other microorganisms, usually epiphytic, but also in the knots. Microorganisms in olive knots either depress *Psu* growth or produce an increase in knot size.

G. Marchi, B. Mori, P. Pollacci, M. Mencuccini, G. Surico Systemic spread of *Pseudomonas savastanoi* pv. *savastanoi* in olive explants. Plant Pathology 58: 152-158 (2009).

G. Marchi, A. Sisto, A. Cimmino, A. Andolfi, M. G. Cipriani, A. Evidente, G. Surico. Interaction between *Pseudomonas savastanoi* pv. *savastanoi* and *Pantoea agglomerans* in olive knots. Plant Pathology 55: 614-624 (2006).

Olive knot is **difficult to control**: the **use of these antagonists as biological control agents** against *Psv* is a promising tool to reduce olive knot incidence on olive crops, following European policy aiming at more sustainable crop production systems (Directive 2009/128/EC) and following the “Guidelines for integrated production of olives” published by IOBC/WPRS

C. Malavolta, D. Perdakis, IOBC Technical Guidelines III. Guidelines for Integrated Production of Olives. IOBC/WPRS Bulletin 77, 1-19 (2012).

We have started studying **the endophytic fungal community associated to *Psv* in the phyllosphere of Portuguese olive tree cultivars**, and their capacity to antagonize *Psv* under ***in vitro* conditions**.

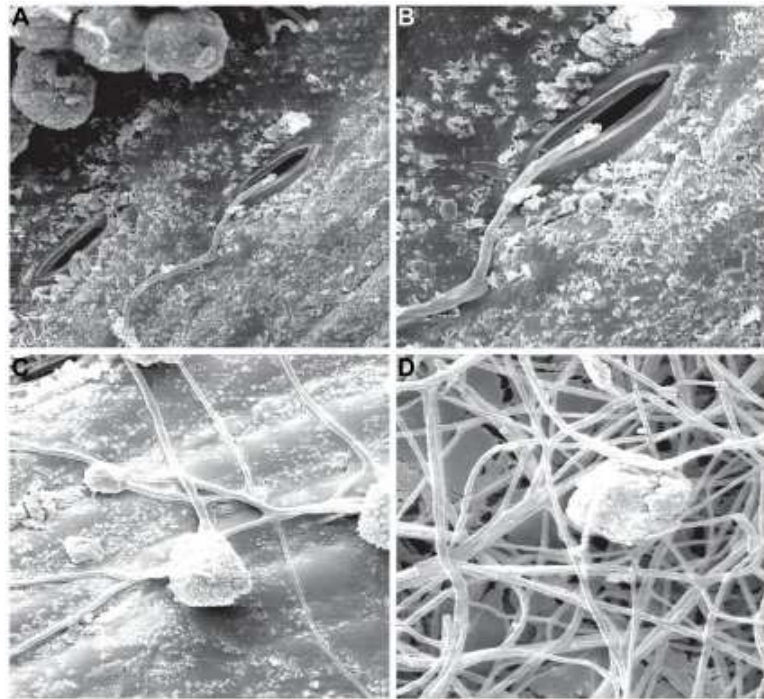


Figure 5: *Epicoccum nigrum*.

Antagonism tested on solid media with agar overlays showed an inhibition zone for the endophyte *Epicoccum nigrum* and its supernatant was showed to reduced *Psv* growth/biomass around 96%, after 48 h of incubation (unpublished data).

This ecological setting shows that in the context of the Olive tree all the three types of mutual relationships, predator-prey, competition and symbiosis simultaneously occur.

Aim: to better understand the effect of the resident fungus (*E. nigrum*) in the *Psv* development.

Mathematical model accounting for the interactions olive tree-*Psv*-*E.nigrum*.

2 The model

Consider a single olive tree affected by the olive knot disease caused by *Psv*. Assume the endophytic fungus *Epicoccum nigrum* present on the olive tree with two effects: positive on the tree, and on the environment, removing bacteria. The endophytic fungus also gains indirectly more space on the plant and directly more food from the plant.

The populations (measurable by biomass - or extent of their surface):

- S : the healthy branches of the olive tree;
- I : the branches of the same olive tree that are infected by bacteria;
- B : the pathogenic bacterium *Psv*, infecting the olive branches;
- N : the endophytic fungus *E. nigrum*, that remove the *Psv* bacterium B , and gets more space and also more nutrients from the plant; they also exert a beneficial effect on the healthy parts of the plant, S .

The model, in which all the parameters represent nonnegative quantities, reads:

$$\begin{aligned}\frac{dS}{dt} &= s \left(1 - \frac{S + I}{K} \right) S - \lambda S B + b N S \\ \frac{dI}{dt} &= \lambda S B - q I B - g I - s \frac{S + I}{K} I \\ \frac{dB}{dt} &= h q I B - a N B - m B - r B^2 \\ \frac{dN}{dt} &= e b N S + u a N B - n N - p N^2.\end{aligned}\tag{1}$$

$$\frac{dS}{dt} = s \left(1 - \frac{S + I}{K} \right) S - \lambda S B + b N S$$

In the first equation the evolution of the tree healthy branches is modeled. They reproduce following a logistic growth, with net biomass production rate s and carrying capacity K and become infected at rate λ by the action of the bacterium. We assume that there is **well mixing of the bacteria in all parts of the tree** because they are transported by the **wind and the rain**. In this way their interaction with the healthy parts of the tree is modeled via a mass action term, this fact in epidemiological terms corresponding to the homogeneous mixing $\lambda S B$. The last term expresses the fact that they get benefit at rate b from the endophytic fungi, with which they have a beneficial relationship.

$$\frac{dI}{dt} = \lambda SB - qIB - gI - s \frac{S + I}{K} I$$

The second equation for the infected branches shows firstly that they become so when they are attacked by the bacterium, secondly they also suffer the action of the bacteria B at rate q , then they experience an additional, disease-related, mortality at rate g and finally are also subject to intraspecific competition for space and nutrients from other healthy and infected branches.

$$\frac{dB}{dt} = hqIB - aNB - mB - rB^2$$

In the third equation we model the bacterium. It gets nutrients from the infected branches, as already mentioned at rate q , with a conversion factor $h < 1$. The second term indicates that they are killed by the *E. nigrum* at rate a , the third one that their natural mortality rate is m . Bacteria can die also by intraspecific competition at rate r .

$$\frac{dN}{dt} = ebNS + uaNB - nN - pN^2.$$

The endophytic fungus is modeled in the fourth equation. They get benefit from their relationship with the healthy branches, at rate b , scaled by a factor $e < 1$, and also by killing the bacterium at rate a , because in this way they get more space for growth, and indirectly also more nutrients. Here $u < 1$ represents another conversion factor. In the last two terms we model their removal from the ecosystem: *Epicoccum nigrum* naturally die at rate n and experience also intraspecific competition at rate p .

3 The ecosystem's steady states

There are the origin $E_0 = (0, 0, 0, 0)$ and the healthy-tree only equilibrium $E_1 = (K, 0, 0, 0)$, which are both always feasible.

The eigenvalues for E_0 are $-g < 0$, $-m < 0$, $-n < 0$ and $s > 0$, showing its **unconditional instability**.

The corresponding eigenvalues of E_1 are $-s < 0$, $-m < 0$, $-g - s < 0$ and $ebK - n$, giving the following condition ensuring the **stability of the equilibrium**:

$$ebK < n. \quad (2)$$

The equilibrium in which the **endophytic fungi are absent**:

$$E_2 = \left(K - \left(1 + \frac{\lambda h q K}{r s} \right) I_2 + \frac{\lambda m K}{r s}, I_2, \frac{h q}{r} I_2 - \frac{m}{r}, 0 \right) \quad (3)$$

where I_2 is the positive root of the quadratic equation:

$$U_2 I_2^2 + V_2 I_2 + Z_2 = 0, \quad V_2 = \frac{\lambda K h q + m q}{r} + 2 \frac{\lambda^2 h q K m}{r^2 s} - g - s, \quad (4)$$

$$U_2 = -\frac{\lambda^2 h^2 q^2 K}{r^2 s} - \frac{h q^2}{r} < 0, \quad Z_2 = -\frac{\lambda K m}{r} - \frac{\lambda^2 m^2 K}{r^2 s} < 0.$$

For a nonnegative root I_2 , by Descartes' rule of signs, we need $V_2 > 0$ and $V_2^2 \geq 4U_2 Z_2$. For nonnegativity of B and S need the conditions:

$$h q I_2 \geq \frac{m}{r}, \quad K + \frac{\lambda m K}{r s} > \left(1 + \frac{\lambda h q K}{r s} \right) I_2$$

Thus **feasibility conditions** are then given by:

$$V_2 > 0, \quad V_2^2 \geq 4U_2 Z_2, \quad \frac{m}{h q} < I_2 < \frac{K(r s + \lambda m)}{r s + \lambda h q K}. \quad (5)$$

The **point with no infection**, the tree is healthy and the phyllosphere microorganisms thrive in it,

$$E_3 = \left(\frac{K(bn - sp)}{Keb^2 - sp}, 0, 0, \frac{s(n - Keb)}{Keb^2 - sp} \right).$$

It is **feasible** if either one of the following sets of conditions holds:

$$\max \left\{ \frac{sp}{n}, \sqrt{\frac{sp}{Ke}} \right\} < b < \frac{n}{Ke} \quad (6)$$

or

$$\frac{n}{Ke} < b < \min \left\{ \frac{sp}{n}, \sqrt{\frac{sp}{Ke}} \right\}. \quad (7)$$

Two of the eigenvalues of $J(E_3)$ are explicit: $-g - sK^{-1}S_3 < 0$, $-m - aN_3 < 0$. The remaining two eigenvalues are the roots of the quadratic equation:

$$\mu^2 - \text{tr}(Q) + \det(Q) = 0$$

with

$$-\text{tr}(Q) = \frac{s}{K}S_3 + pN_3 > 0, \quad \det(Q) = \frac{s}{K}pS_3N_3 - b^2eS_3N_3.$$

Stability of E_3 requires that $\det(Q) > 0$, that is:

$$sp > Kb^2e. \quad (8)$$

Condition (6) is the opposite of (8), so that in this case E_3 is feasible but unstable.

If instead (7) holds, (8) is verified and E_3 is stable.

Moreover, there is a transcritical bifurcation between E_1 and E_3 , compare the stability condition (2) of E_1 with the feasibility condition (7) for E_3 .

Finally, the **coexistence equilibrium** is found as follows:

$$E^* = \left(\frac{sK - sI^* - k\lambda B^* + KbN^*}{s}, I^*, B^*, \frac{hqI^* - rB^* - m}{a} \right), \quad (9)$$

and where I^* solves a quadratic equation with known A_B , A_C and A_I :

$$I_1^* = \frac{b^*r + m}{hq} > 0, \quad I_2^* = \frac{A_B B^* + A_C}{A_I}. \quad (10)$$

But **focusing only on I_1^*** , B^* solves the quadratic with known coefficients

$$U_1 B^{*2} + V_1 B^* + Z_1 = 0. \quad (11)$$

The quadratic equation (11) has **real roots if and only if $V_1^2 - 4U_1 Z_1 \geq 0$** .

For **just one positive value** of B^* , need exactly one sign variation, **ensured by one of the alternative situations: $U_1 V_1 < 0$ or $V_1 Z_1 < 0$ or $U_1 Z_1 < 0$** .

If instead U_1 and Z_1 have the same sign and V_1 the opposite one, both roots of (11) are positive.

In summary, feasibility of E^* :

$$sK + KbN^* > sI^* + K\lambda B^*, \quad hqI^* > rB^* + m, \quad V_1^2 - 4U_1Z_1 \geq 0. \quad (12)$$

Stability for equilibrium with no endophytes E_2 and for the coexistence equilibrium E^* is investigated numerically.

4 Numerical simulations

The ecosystem (1) embeds a symbiotic subsystem for S and N . This classical two-populations mathematical model can lead to unbounded, ecologically unrealistic, growth, if its isoclines are suitably chosen. To avoid this need assumptions on the ecosystem parameters.

The symbiotic subsystem isoclines

$$s - \frac{s}{K}S + bN = 0, \quad ebS - n - pN = 0 \quad (13)$$

intersect at the point

$$\left(\frac{K(nb - sp)}{Keb^2 - sp}, \quad \frac{s}{b} \left(-1 + \frac{nb - sp}{Keb^2 - sp} \right) \right), \quad (14)$$

feasible if the two sets of alternative feasibility conditions for E_3 hold (6) and (7).

Goal: want to control the spread of the disease in the olive tree.

For the parameters a and m , we use the fixed values $m = 0.183$ (the time unit is taken to be hours) and $a = 0.021$ (time unit hours) provided by our laboratory experiments, yet unpublished.

The parameter b is not experimentally known and thus it is chosen to satisfy the conditions (6) and (7).

To run the simulations, the intrinsic ode45 routine of Matlab2016a and the bifurcation software XPPAUT are used. Set of parameters reference values:

$$\begin{aligned} s &= 4.24476, & b &= 0.2, & q &= 9.24772, & g &= 6.42079, & (15) \\ h &= 0.226653, & m &= 0.183, & a &= 0.021, & e &= 0.9, \\ n &= 1.045, & u &= 0.214479, & K &= 50, & r &= 3.95804, & p &= 0.8 \end{aligned}$$

Initial conditions

$$S(0) = 7.0300, \quad I(0) = 7.5415, \quad B(0) = 5.4729, \quad N(0) = 5.5348. \quad (16)$$

Scenarios obtained varying mainly the infection rate parameter λ .

Construct the one-parameter bifurcation diagrams for the four populations S , I , B and N , Figs. 4 and 4. In view of the constraints (6) and (7), the parameter b can lie only in the approximate range $[0.023, 0.2747]$.

In the first diagram for the population S , one can see that for $0.5 \lesssim \lambda \lesssim 11.86$ five equilibrium points are feasible: for $0.5 \lesssim \lambda \lesssim 4.83$ one of the two coexistence equilibria is stable, given by the red line (b), while the black lines (a), (c), (d) denote the unstable equilibria. The same equilibrium points can be noted in the other bifurcation diagrams for I , B and N , denoted with the same letters.

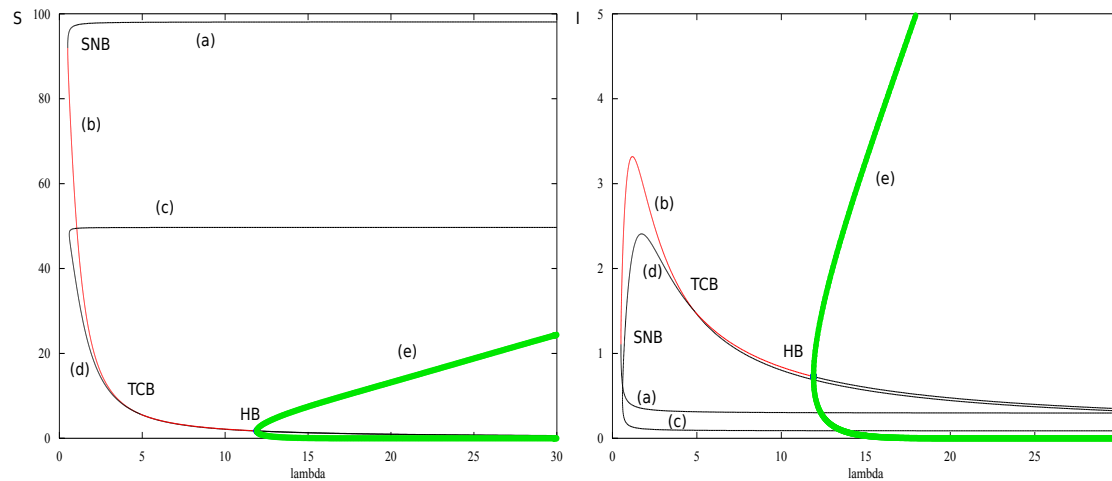


Figure 6: Left: bifurcation diagram (λ, S) . Right: bifurcation diagram (λ, I) . Parameter values: $s = 4.24476$, $b = 0.2$, $q = 9.24772$, $g = 6.42079$, $h = 0.226653$, $m = 0.183$, $a = 0.021$, $e = 0.9$, $u = 0.214479$, $n = 1.045$, $K = 50$, $r = 3.95804$, $p = 0.8$. Initial conditions: $S(0) = 7.0300$, $I(0) = 7.5415$, $B(0) = 5.4729$, $N(0) = 5.5348$. HB: Hopf bifurcation point. TCB: transcritical bifurcation point. SNB: saddle-node bifurcation point. (a), (b), (c), (d): equilibrium points. (e): stable limit cycle.

In the second diagram of Fig. 4, for $\lambda \gtrsim 4.83$, the population N collapses to 0 and E_2 , the line (d), becomes stable after a transcritical bifurcation (TCB), which occurs between (b) and (d) for $\lambda \cong 4.83$. A saddle-node bifurcation (SNB) occurring at $\lambda \cong 0.5$ separates the stable coexistence equilibrium (b) from the unstable one, denoted with (a). For values of λ larger than 11.86, the three nonvanishing populations S , I and B in the solution of the system (1) oscillate, due to the presence of a stable limit cycle, whose maximum and minimum values are plotted by the line named (e). The Hopf bifurcation from which the limit cycle originates occurs for $\lambda \cong 11.9$ (HB). At $\lambda \cong 11.86$, another Hopf bifurcation leads to the presence of an unstable limit cycle, surrounding the stable one. For simplicity, here it is not represented into the bifurcation diagrams in order not to clutter the figures.

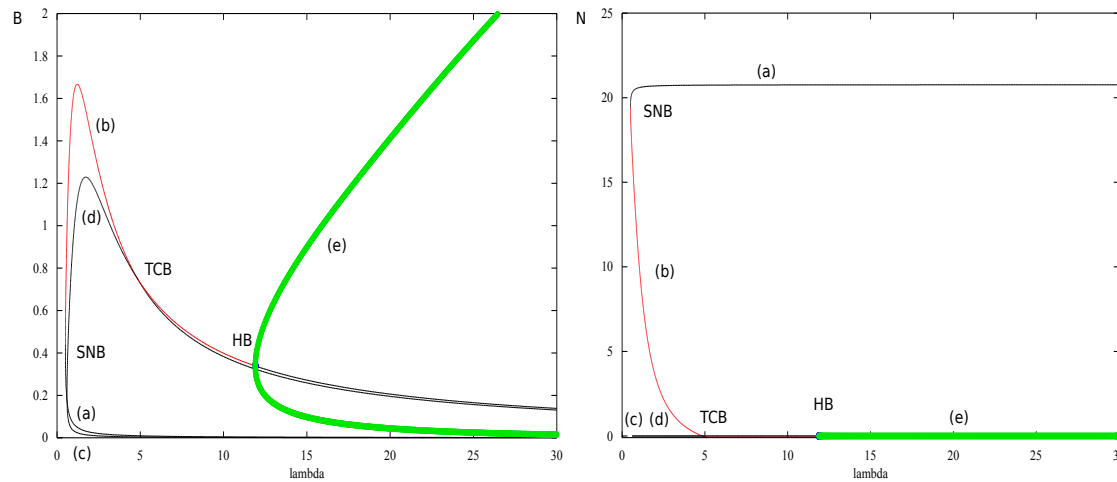


Figure 7: Left: bifurcation diagram (λ, B) . Right: bifurcation diagram (λ, N) . Parameter values: $s = 4.24476$, $b = 0.2$, $q = 9.24772$, $g = 6.42079$, $h = 0.226653$, $m = 0.183$, $a = 0.021$, $e = 0.9$, $u = 0.214479$, $n = 1.045$, $K = 50$, $r = 3.95804$, $p = 0.8$. Initial conditions: $S(0) = 7.0300$, $I(0) = 7.5415$, $B(0) = 5.4729$, $N(0) = 5.5348$. HB: Hopf bifurcation point. TCB: transcritical bifurcation point. SNB: saddle-node bifurcation point. (a), (b), (c), (d): equilibrium points. (e): stable limit cycle.

Fig. 4 shows the results for higher values of λ , namely for $\lambda = 55$. The solutions for S , I and N according to continuous time are characterized by high amplitude oscillations, approaching values dangerously close to zero, while the N population rapidly decays and ultimately vanishes.

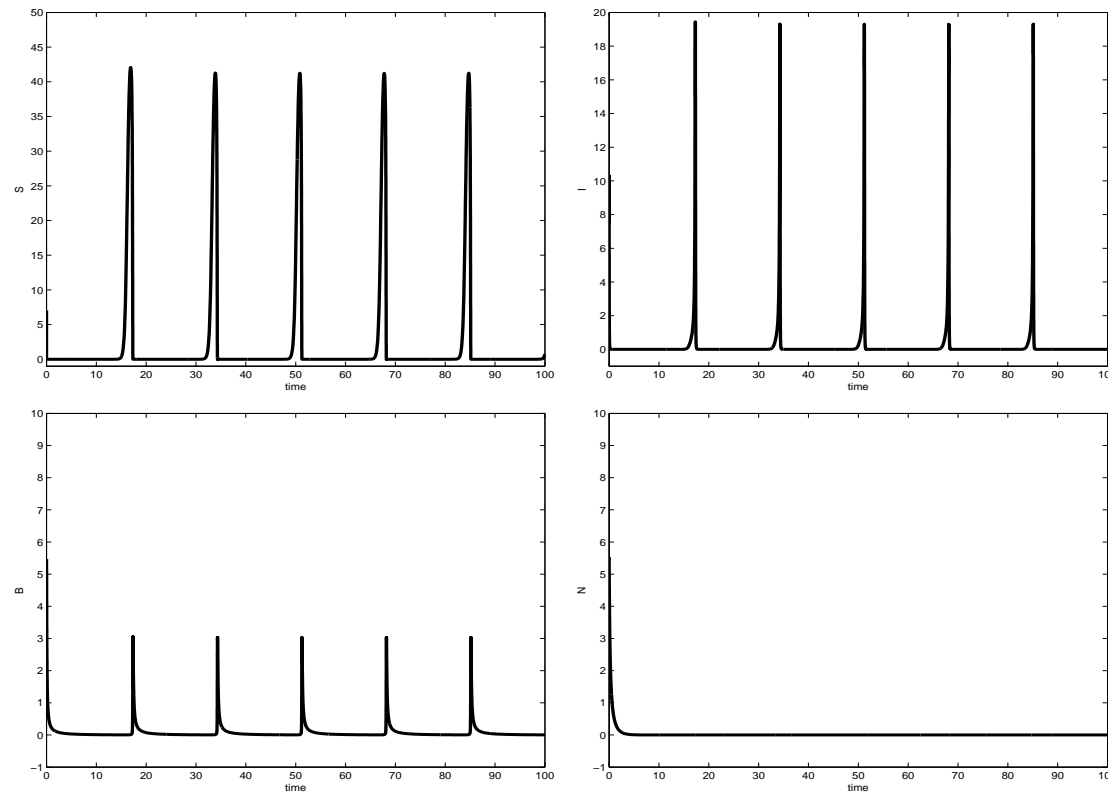


Figure 8: Parameter values: $\lambda = 55$, $s = 4.24476$, $b = 0.2$, $q = 9.24772$, $g = 6.42079$, $h = 0.226653$, $m = 0.183$, $a = 0.021$, $e = 0.9$, $u = 0.214479$, $n = 1.045$, $K = 50$, $r = 3.95804$, $p = 0.8$. Initial conditions: $S(0) = 7.0300$, $I(0) = 7.5415$, $B(0) = 5.4729$, $N(0) = 5.5348$. Note that the zero value is located at higher level than the frames' bottom

In Fig. 4 the trajectories for $\lambda = 0.2$ are shown: we note that for values of λ smaller than about 0.5 the system converges to the equilibrium point E_3 . Consequently the disease is eradicated due to the low value of the transmission rate. The healthy branches population thrives to very high levels, higher than the carrying capacity, because of the beneficial effect of the endophytic fungus.

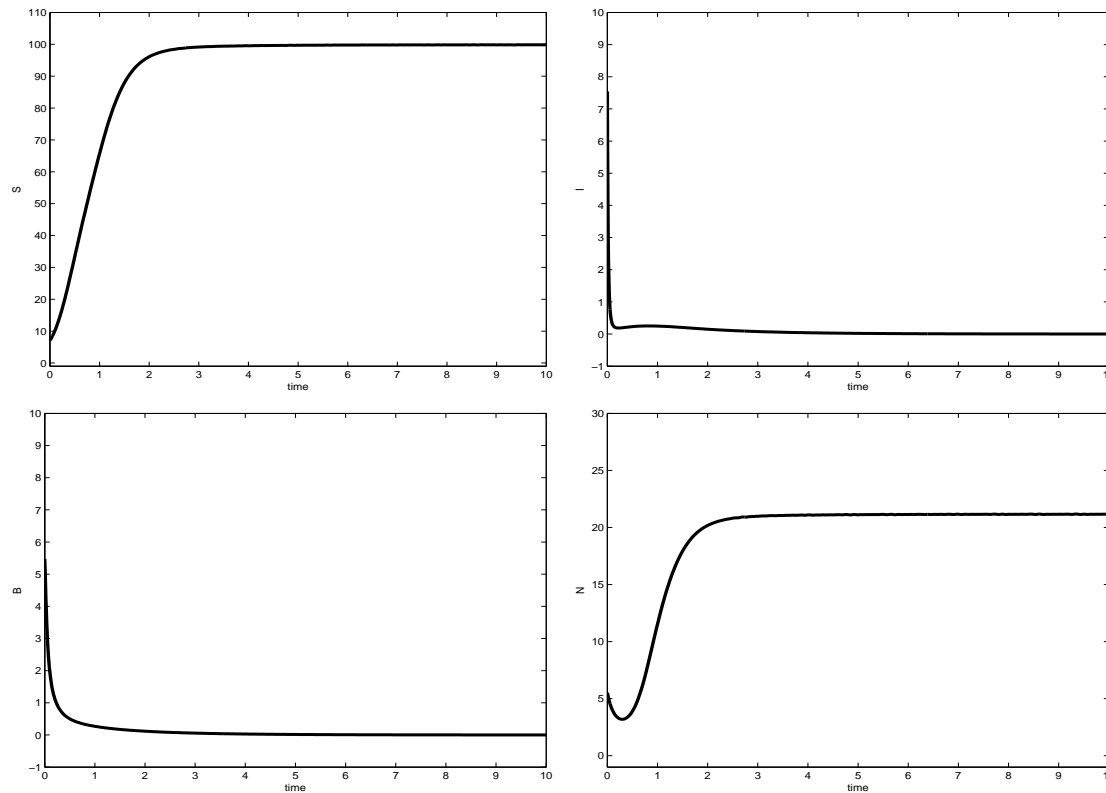


Figure 9: Parameter values: $\lambda = 0.2$, $s = 4.24476$, $b = 0.2$, $q = 9.24772$, $g = 6.42079$, $h = 0.226653$, $m = 0.183$, $a = 0.021$, $e = 0.9$, $u = 0.214479$, $n = 1.045$, $K = 50$, $r = 3.95804$, $p = 0.8$. Initial conditions: $S(0) = 7.0300$, $I(0) = 7.5415$, $B(0) = 5.4729$, $N(0) = 5.5348$. Note that both infected branches and bacteria disappear, the zero value is indeed located at higher level than the frames' bottom.

Equilibria sensitivity analysis to variations in two parameters: e.g. effects due to climate changes inducing substantial changes in the ecosystem.

Firstly, Fig. 4 for the pair $\lambda - g$, where g is the additional disease-related mortality rate of the infected part of the plant. Use same set of parameters and IC's of Figs. 4 and 4, but allow the ranges $\lambda \in [0, 10]$ and $g \in [0, 10]$. The surfaces represent each population level at equilibrium.

For low λ and g higher than 6, I and B vanish, while S and N thrive at rather high levels: here E_3 is stable, the disease is thus eradicated.

This is sensible, the disease propagation rate is low and the rate at which the infected part of the plant die is high, in turn damaging the bacteria in the plant and removing the infected branches.

For low values of both g and λ instead we find coexistence and when $\lambda \gtrsim 4.83$, the population of the endophytic fungi, N , disappears, with the ecosystem attaining the endophytic fungi-free equilibrium E_2 , but with alarmingly small values of the healthy parts of the plant.

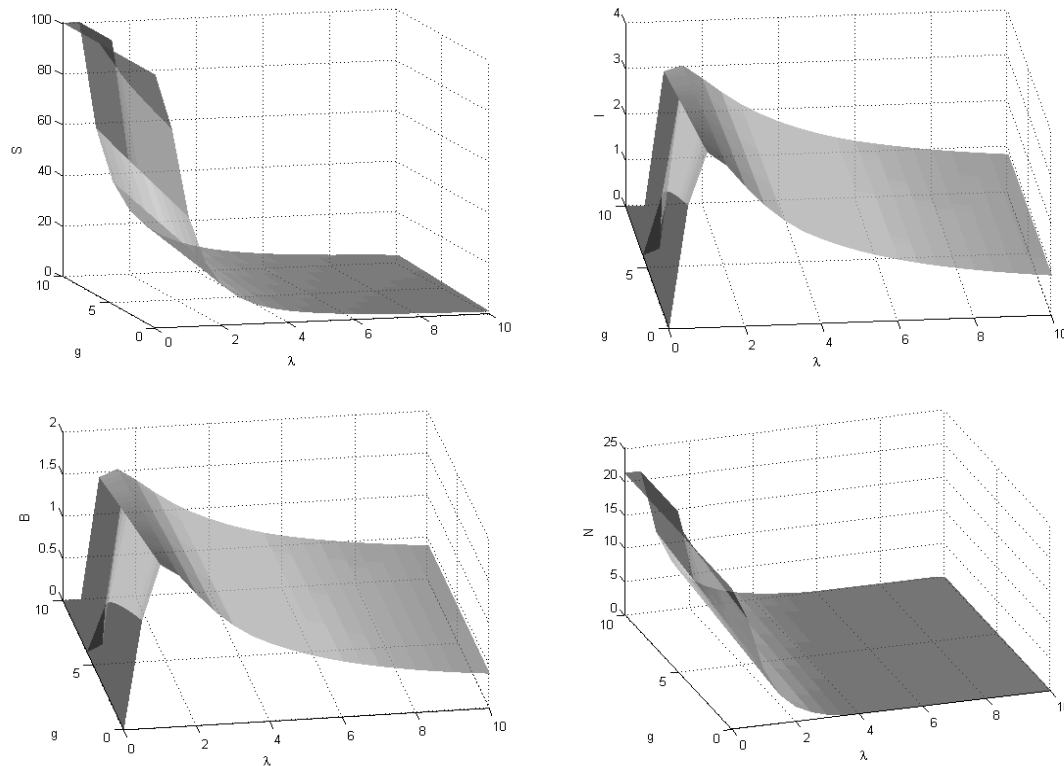


Figure 10: Populations as functions of λ and g . Remaining parameter values: $s = 4.24476$, $b = 0.2$, $q = 9.24772$, $h = 0.226653$, $m = 0.183$, $a = 0.021$, $e = 0.9$, $u = 0.214479$, $n = 1.045$, $K = 50$, $r = 3.95804$, $p = 0.8$. Initial conditions: $S(0) = 7.0300$, $I(0) = 7.5415$, $B(0) = 5.4729$, $N(0) = 5.5348$.

Then, Fig. 4, consider the transmission rate and the rate at which the antagonistic fungi produce a beneficial effect on the plant, i.e. $\lambda - b$, in $[0, 11] \times [0.023, 0.2747]$. For b , impose the feasibility for E_3 , namely (6) and (7). E_3 is attained when $\lambda < 0.5$, matching the analytical results and also the results of the one-parameter bifurcation diagram in Figs. 4 and 4.

Bacteria and infected parts of the plant vanish, only healthy branches and antagonistic fungi thrive. For low b the two species present in the system assume low values, while for $b > 0.25$ they increase to biologically considerable high values.

In Fig. 4 for $0.5 \lesssim \lambda \lesssim 4.83$ the system converges to coexistence: N is very close to zero. For $\lambda \gtrsim 4.83$, instead E_2 with no endophytic fungus *Epicoccum nigrum* becomes stable. When $\lambda \approx 4.83$ and $b \approx 0.2747$ the infected branches and bacteria populations I and B have a peak, while S and N rapidly drop to values close to zero.

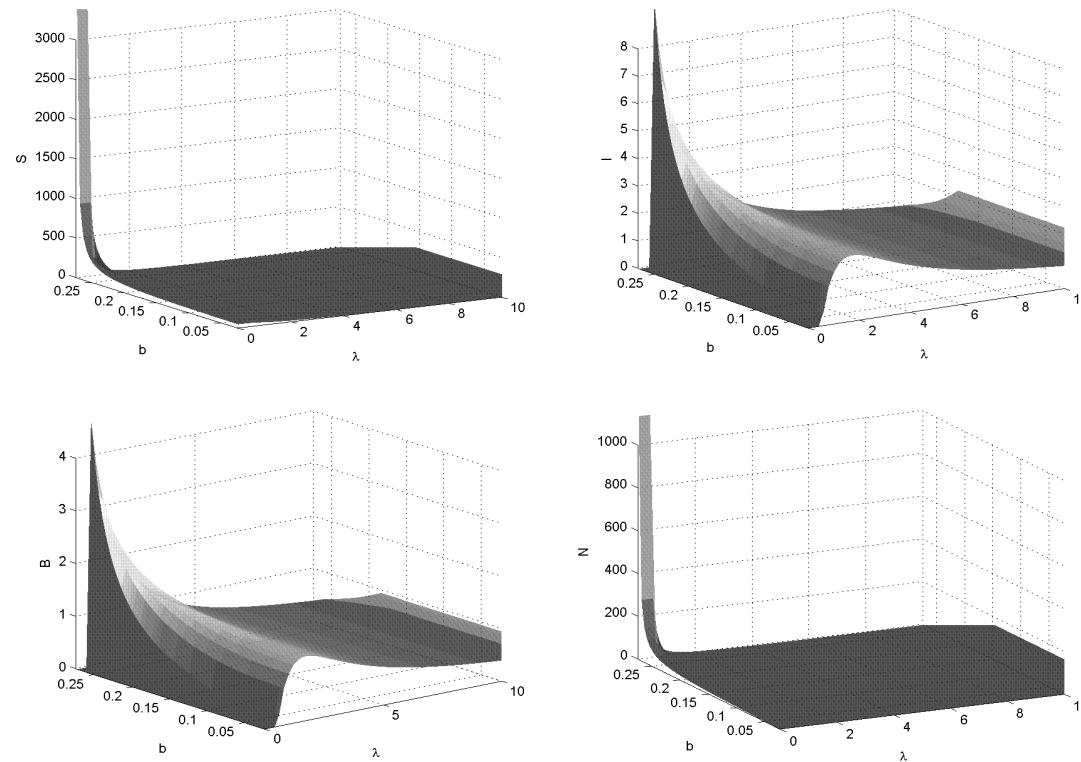


Figure 11: Populations as functions of λ and b . Remaining parameter values: $s = 4.24476$, $q = 9.24772$, $g = 6.42079$, $h = 0.226653$, $m = 0.183$, $a = 0.021$, $e = 0.9$, $u = 0.214479$, $n = 1.045$, $K = 50$, $r = 3.95804$, $p = 0.8$. Initial conditions: $S = 7.0300$, $I = 7.5415$, $B = 5.4729$, $N = 5.5348$.

We finally consider the parameter pair $\lambda - q$, recalling that the latter represents the mortality rate of the infected branches due to the attack of the bacteria.

Keeping the previously chosen set of the parameters (15), for values of $\lambda > 11.9$, the system converges to a stable limit cycle, in which however the endophytic fungi population N vanishes. Fig. 4 shows the system solutions as functions of time for $\lambda = 20 > 11.9$ and $q = 5, q = 8, q = 25$.

Note that the change in the values of the disease-related mortality rate q of the infected branches does not affect the feasibility and stability of the equilibrium, but it rather influences the amplitude of the oscillations, which decreases for higher values of q .

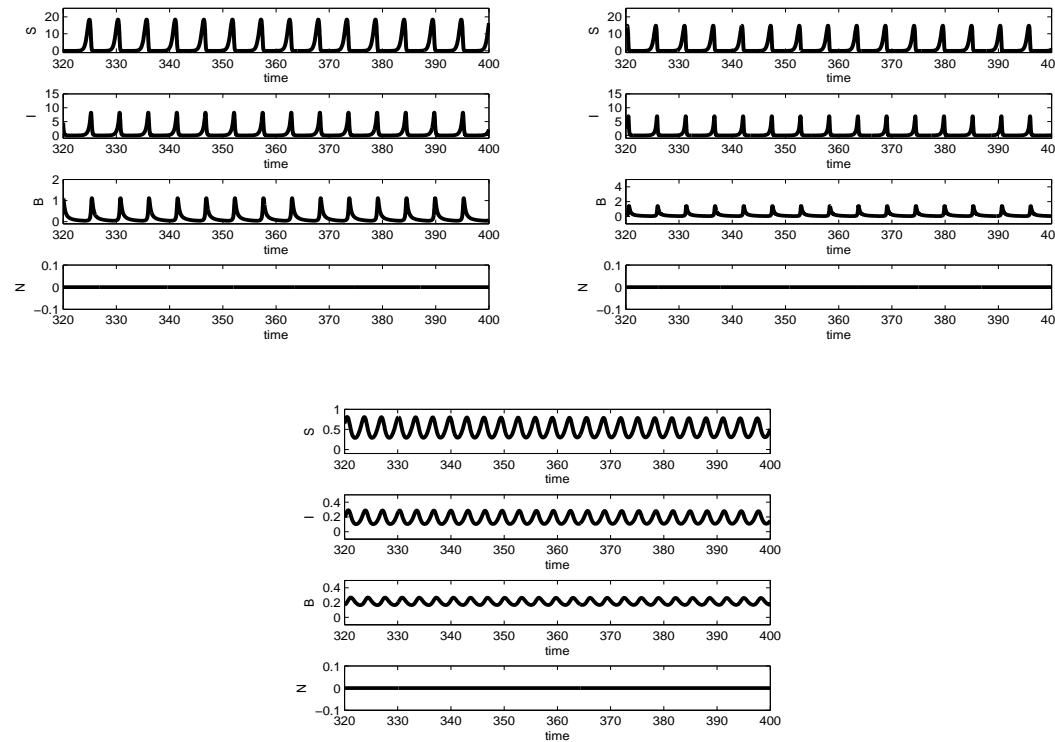


Figure 12: Persistent limit cycles of the system. Top, left: $q = 5$. Top, right: $q = 8$. Bottom: $q = 25$. Remaining parameters values: $\lambda = 20$, $s = 4.24476$, $b = 0.2$, $g = 6.42079$, $h = 0.226653$, $m = 0.183$, $a = 0.021$, $e = 0.9$, $u = 0.214479$, $n = 1.045$, $K = 50$, $r = 3.95804$, $p = 0.8$. Initial conditions: $S = 7.0300$, $I = 7.5415$, $B = 5.4729$, $N = 5.5348$.

Note that the solutions are plotted for time values in the range $[320, 400]$.

Fig. 4, shows the system behavior in terms of the variations of the parameter q in the range $[0, 20]$, together with the influence of the disease transmission coefficient $\lambda \in [0, 20]$.

For low values of the parameter q , independently of the value of λ , the system settles to the disease-free equilibrium E_3 , with the presence of only the healthy part of the plant and the antagonistic endophytic fungi.

In a region close to the origin the favorable equilibrium point E_3 is stable.

For higher values of q and $\lambda \gtrsim 0.5$, the system achieves coexistence at steady values, with S and N showing a quick decrease toward zero.

Finally, larger values of λ and q lead the system to reach the equilibrium point E_2 , with the presence of the disease and the infected branches, together with the healthy branches, where the endophytic fungi disappear.

For even larger values of $\lambda > 11.9$, the ecosystem starts to oscillate. The surfaces with the highest and lowest peaks in the limit cycles are shown for the populations S , I and B while N disappears.

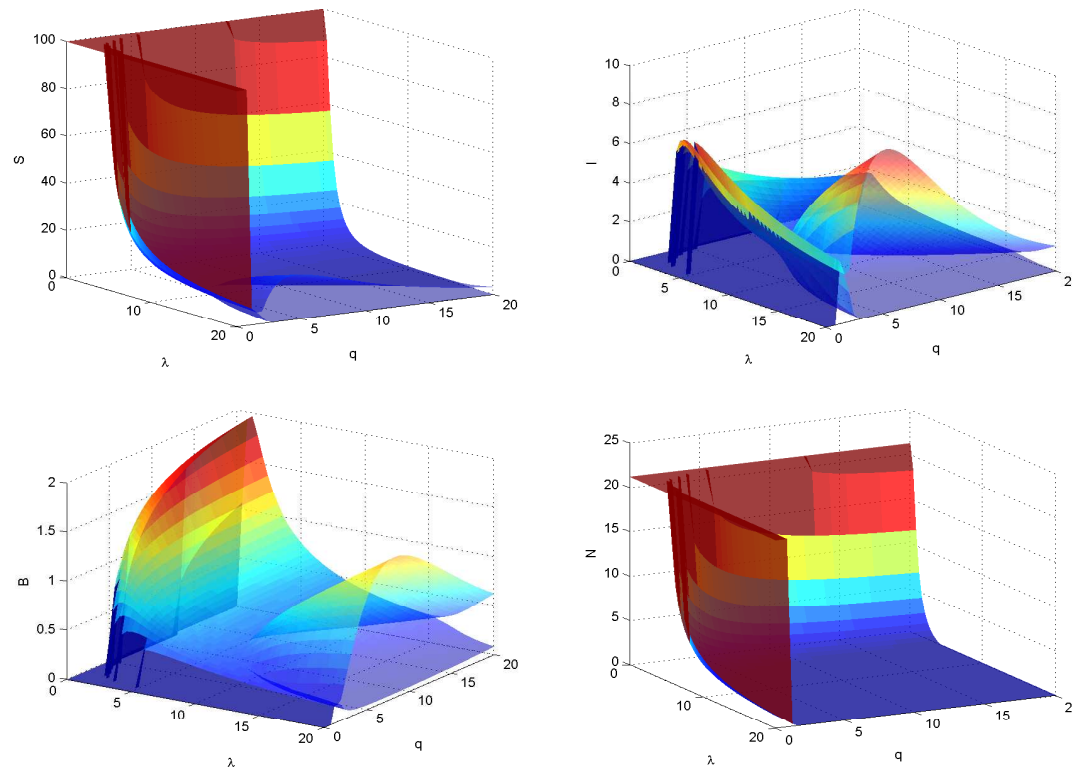


Figure 13: Populations as functions of λ and q . Remaining parameter values: $s = 4.24476$, $g = 6.42079$, $h = 0.226653$, $m = 0.183$, $a = 0.021$, $e = 0.9$, $u = 0.214479$, $n = 1.045$, $K = 50$, $r = 3.95804$, $p = 0.8$, $b = 0.2$. Initial conditions: $S = 7.0300$, $I = 7.5415$, $B = 5.4729$, $N = 5.5348$.

5 Conclusions

Proposed a model for fighting by natural means harmful bacteria harboring in the olive trees.

The disease-free equilibrium E_3 is biologically the most relevant one, healthy branches and the endophytic fungi survive, while the infected parts of the plant and the bacterium P_{sv} disappear. The plant benefits from the symbiotic action of the fungi, in that it thrives better, at higher levels, as shown in Fig. 4. However, to achieve this, the parameter b must satisfy the condition (7), to have E_3 both feasible and stable, which is a very narrow range of values for b . In other words, the benefit that the endophytic fungi exert on the tree must be confined to a certain appropriate range.

The disease-and-endophytic fungi-free equilibrium point E_1 is also good for the plant, since it ensures anyway the survival of the healthy part of the olive tree plant. Here, with no help from the endophytic fungi, the branches attain just their own carrying capacity.

There are equilibria that must possibly be avoided, E_2 and E^* because they still harbor the harmful bacteria, because at E_2 the endemic endophytic fungi-free equilibrium vanish, not good since they provide an effective suppression mechanism for *Psv* bacteria's growth.

A highly virulent disease, with large transmission coefficient, leads to populations oscillations that are extremely close to vanishing levels, see Fig. 4, that due to stochastic environmental fluctuations may lead to ecosystem collapse i.e. to the tree's death.

An additional difficulty for obtaining a stable disease-free equilibrium is the fact that the disease transmission rate λ must lie in a very small low range. From Fig. 4, the additional disease-related mortality rate must also be high, because infected branches are fast removed before bacteria can replicate.

A final point is that also the disease-and-endophytic fungi-free equilibrium point E_1 is difficult to be achieved in practice: the stability condition hinges on high values of the parameter n , the fungi mortality, which is however known in general to be quite small.

The findings on the sensitivity analysis however indicate that a high infected branch mortality g helps in controlling the disease. This can also be achieved by human-related external means, like pruning of the leaves and branches that appear to be disease-affected.